DISCRETE MATHEMATICS IN RELATION TO COMPUTER SCIENCE

The Determination of Distances between Images by de Rham Currents Method

S. N. Chukanov[1]

[1]Sobolev Institute of Mathematics, SB RAS, Omsk branch, 13 Pevtsova str., Omsk 644043, Russia.

The goal of the paper is to develop an algorithm for matching the shapes of images of objects based on the geometric method of de Rham currents and preliminary affine transformation of the source image shape. In the formation of the matching algorithm, the problems of ensuring invariance to geometric image transformations and ensuring the absence of a bijective correspondence requirement between images segments were solved. The algorithm of shapes matching based on the current method is resistant to changes of the topology of object shapes and reparametrization. When analyzing the data structures of an object, not only the geometric form is important, but also the signals associated with this form by functional dependence. To take these signals into account, it is proposed to expand de Rham currents with an additional component corresponding to the signal structure. To improve the accuracy of shapes matching of the source and terminal images we determine the functional on the basis of the formation of a squared distance between the shapes of the source and terminal images modeled by de Rham currents. The original image is subjected to preliminary affine transformation to minimize the squared distance between the deformed and terminal images.

Keywords: pattern recognition; image matching; de Rham current; affine transformations

INFORMATION ABOUT THE AUTHORS

Sergey N. Chukanov | orcid.org/0000-0002-8106-9813. E-mail: ch_sn@mail.ru
Doctor of Technical Science, Professor.

For citation: S. N. Chukanov, "The Determination of Distances between Images by de Rham Currents Method", *Modeling and analysis of information systems*, vol. 27, no. 1, pp. 96-107, 2020.

DISCRETE MATHEMATICS IN RELATION TO COMPUTER SCIENCE

Определение расстояний между изображениями методом потоков де Рама

С. Н. Чуканов[1]

[1]Институт математики им. С. Л. Соболева СО РАН, Омский филиал, ул. Певцова, 13, г. Омск, 644043, Россия.

Целью работы является разработка алгоритма сравнения форм изображений объектов, основанного на геометрическом методе потоков де Рама и предварительном аффинном преобразовании исходной формы изображения. При формировании алгоритма сравнения решены задачи обеспечения инвариантности к геометрическим преобразованиям изображений и обеспечения отсутствия требования биективного соответствия между сегментами исходного и терминального изображений. Алгоритм сравнения форм, основанный на методе потоков, устойчив к изменению топологии форм объектов и репараметризации. При анализе структур данных объекта имеет значение не только геометрическая форма, но и сигналы, ассоциированные с этой формой функциональной зависимостью. Для учета этих сигналов предлагается расширить потоки де Рама дополнительным компонентом, соответствующим структуре сигнала. Для повышения точности сравнения форм исходного и терминального изображений определяется функционал на основе формирования квадрата расстояния между формами исходного и терминального изображений, моделируемыми потоками де Рама. Исходное изображение подвергается предварительному аффинному преобразованию для минимизации квадрата расстояния между деформированным и терминальным изображениями.

Ключевые слова: распознавание образов; сравнение изображений; поток де Рама; аффинные преобразования

ИНФОРМАЦИЯ ОБ АВТОРАХ

Сергей Николаевич Чуканов | orcid.org/0000-0002-8106-9813. E-mail: ch_sn@mail.ru
д-р техн. наук, профессор.

Introduction

Analysis and matching of image shapes of objects is an important problem in pattern recognition [1], image registration [2], biometrics [3], computational anatomy [4]. The determination of distances for matching the shapes of objects is one of the methods for analyzing shapes in pattern recognition. Known distances used in pattern recognition are: Hausdorff, Frechet, Procrustes, Wasserstein and others [5]. One of the most effective methods for matching the shapes of objects is the LDDMM method (Large deformation diffeomorphic metric mapping [6]), in which the distance between the shapes is determined by the minimized functional consisting of the integral of the deformation energy of the original image and the terminal and the sum squared of deviations between the resulting deformable and terminal image.

The traditional methods of matching image shapes in pattern recognition problems have the following disadvantages. Firstly, the lack of invariance of methods in affine transformations of the shapes of images of objects; secondly, the requirement of bijective correspondence between image segments; thirdly, the lack of accounting of the orientation of the shapes of the source and terminal images; fourthly, the lack of accounting of the functional dependence of image segments.

1. Problem statement

Purpose of this paper is to develop an algorithm for matching the image shapes of objects, which is devoid of the above disadvantages. An algorithm for matching shapes based on the geometric de Rham current method [7] and preliminary affine transformation of the original image form is proposed. The method of currents can be used to represent and analyze forms of various nature: point landmarks, curves, surfaces, signals. If $\Omega^k(M)$ is the space of continuous differential k-forms ω in $M \in \mathbb{R}^d$, then the space of de Rham k-currents $\left(\Omega^k\right)^*(M)$ is the dual space to the space $\Omega^k(M)$; k-current $T(\cdot) \in \left(\Omega^k\right)^*(M)$ is a linear functional mapping a differential k-form $\omega \in \Omega^k(M)$: $\omega \to T(\omega) \in \mathbb{R}$. For any hypersurface $S \in \mathbb{R}^k$ we can associate such current $T_S(\cdot) \in \left(\Omega^k\right)^*$ that [7]:

$$T_S(\omega) \in \int_S \omega \in; \forall \omega \in \Omega^k.$$

In the formation of the matching algorithm, the following problems were solved: ensuring the invariance to geometric image transformations, ensuring the absence of a bijective correspondence requirement between image segments [8–10]. Using the de Rham current algorithm allow us to increase the accuracy of matching by taking into account the orientation of the segments of the image shape. The algorithm for matching shapes based on the current method is stable when changing the topology of the shapes of objects and changing parameterization.

The problem of correctly determination the distance between currents that decode the shapes of objects is solved by imbedding the space of de Rham currents in RKHS (reproducing kernel Hilbert spaces) [11]. The study of the shapes of objects is proposed to be carried out by forming test vector fields. Since the de Rham current is not a scalar, for working with currents it is necessary to use vector-valued RKHS [12, 13].

When analyzing the data structures of an object, not only the geometric shape is important, but also the signals associated with this shape with functional dependence. Signals can include structures that are more complicated than real numbers; e.g. vector, tensor signals, quaternions, etc. To take these signals into account, it is proposed to expand de Rham currents with an additional component corresponding to the signal structure.

The results of a diffeomorphic matching of the shapes of objects with an extension of the LDDMM algorithm to the case of metamorphosis, in which there may be no bijective correspondence between the segments of the source and final images, are presented in the article [14]. In this case, a functional is formed that corresponds to the image deformation and determines the distance between the shapes of the initial and terminal images. In order to increase the accuracy of matching the shapes of the source and terminal images in this paper, we determine the functional on the basis of the formation of the squared distance

between the shapes of the source and terminal images modeled by de Rham currents. The source image undergoes a preliminary affine transformation formalized by Lie groups to minimize the squared distance between the two shapes. The minimization of the functional of the squared distance between the image shapes constructed using de Rham currents is based on the QPSO algorithm.

2. Hamiltonian mechanics of image points

Representation of an image after a diffeomorphic transformation can be considered as an evolution of point landmarks of an image based on the principles of Hamilton mechanics. Consider the parameterization of the image by particles. Let $q_i(t)$; $i = 1, \ldots, N$ be the position vector of the particle i and $p_i(t)$; $i = 1, \ldots, N$ be the corresponding momentum vector in time t. If we assume that the moments and velocities of particles are interconnected by the relation: $p_i = \mathcal{L} \cdot v_i$, where $\mathcal{L}$ is an invertible linear operator, then the inverse operator $\mathcal{L}^{-1}$: $v_i = \mathcal{L}^{-1} \cdot p_i = \mathcal{K}p_i$. For an operator $\mathcal{L} = \mathrm{id} - \alpha\nabla^2$ in space $\mathbb{R}^2$, the inverse operator $\mathcal{K} = \mathcal{L}^{-1}$ can be approximated by the Gauss function: $K\left(q_i - q_j\right) = \beta e^{-\alpha^{-2}\left(q_i-q_j\right)^T\left(q_i-q_j\right)}$.

We construct a functional J_0 corresponding to the deformation of the image represented by a set of points:

$$J_0 = \frac{1}{2}\int\limits_0^1 \left\{ \sum_{i,j=1}^N p_i^T K\left(q_i - q_j\right) p_j \right\} dt.$$

Minimization J_0 is carried out according to the values of the components of the momentum vectors p_i, p_j; $i, j = 1 \ldots N$. The minimization problem for J_0 can be represented as the optimal control problem with the Hamiltonian: $H_0(q, p) = \frac{1}{2}\sum_{i,j=1}^N p_i^T K\left(q_i - q_j\right) p_j$. If the Hamiltonian of the system is taken in the form:

$$H(q, p) = H_0(q, p) + \sigma^{-2}\sum_{i=1}^N \left(\dot{q}_i - v_i(q)\right)^2,$$

then the Hamilton equations for derivatives $\dot{\mathbf{p}} = (\dot{p}_1, \ldots, \dot{p}_N)$, $\dot{\mathbf{q}} = (\dot{q}_1, \ldots, \dot{q}_N)$ will take the form [14] :

$$\begin{aligned}
\dot{p}_i &= -\frac{\partial H}{\partial q_i} = -\sum_{j=1}^N p_i^T \nabla_{q_i} K\left(q_i - q_j\right) p_j; \\
\dot{q}_i &= \frac{\partial H}{\partial p_i} = \sum_{j=1}^N K\left(q_i - q_j\right) p_j + \sigma^2 p_i.
\end{aligned} \tag{1}$$

3. Matching the shapes of objects

The theory of currents was developed by G. de Rham [7]. The denomination "current" is chosen by analogy with electromagnetism. For example, in accordance with the law of induction of M. Faraday, the intensity of the current in the wire loop caused by a change in the magnetic field is proportional to the change in the flux of this magnetic field through the surface bounded by the loop. This means that if you measure the current strength in the wire for all possible changes in the magnetic field, you can get the loop geometry. In the works [15–17] presents the concept of currents for the formation of a measure of the difference between simplicial complexes, which does not imply a bijective correspondence between the structures of objects. The concept of using currents is to study the shape of objects by forming test vector fields.

Let $\Omega^k(M)$ be the space of continuous differential k-forms ω in $M \in \mathbb{R}^d$. The space of k-currents is the dual space to the space of differential k-forms; k-current is a linear functional mapping a differential k-form ω: $\omega \to T(\omega) \in \mathbb{R}$. The form $\omega \in \Omega^{n-1}$ can be integrated over a hypersurface S, which is associated with $(n-1)$-current $T_S \in (\Omega^*)^{n-1}$ in such a way that: $T_S(\omega) = \int\limits_S \omega, \forall \omega \in \Omega^{n-1}$. Suppose that a hypersurface S is

parameterized by a surface $r\colon D \subset \mathbb{R}^{n-1} \to \mathbb{R}^n$, with $r(D) = S$. Then:

$$T_S(\omega) = \int\limits_S \omega = \int\limits_D \omega(r(x)) \left(r_{x_1} \wedge \ldots \wedge r_{x_{n-1}}\right) dx_1 \ldots dx_{n-1},$$

where $r_{x_i} = \dfrac{\partial r}{\partial x_i}$; $i = 1, \ldots, n-1$.

Consider the case of plane closed curves and compact surfaces. Let $l\colon L = [a, b] \to \mathbb{R}^2$ be a parametrized curve in $\mathbb{R}^2$. We associate with l such a current $T_l(\cdot)$ that when $T_l(\cdot)$ acting on ω we get: $T_l(\omega) = \int\limits_L (\bar{\omega}(l(t)) \cdot \tau(t)) \frac{\partial l(t)}{\partial t} dt$, where $\tau(t)$ is the tangent vector to l at the point t, $\bar{\omega}$ is the vector field in $\mathbb{R}^2$ corresponding ω. Let S be a surface in $\mathbb{R}^3$, with parameterization $r\colon (u, v) \subset \mathbb{R}^2 \to \mathbb{R}^3$; $r(u, v) = S$. We associate with S such a current $T_S(\cdot)$ that when acting $T_S(\cdot)$ on ω we get: $T_S(\omega) = \int\limits_U \bar{\omega}(r(u, v)) \cdot (r_u \times r_u) \, du \, dv$, where $\bar{\omega}$ is the vector field in $\mathbb{R}^3$, corresponding to ω, "$\times$" is the vector product operator.

Let $(W, \langle \cdot, \cdot \rangle_W)$ be a test Hilbert space of vector fields $\mathbb{R}^n \to \mathbb{R}^n$. We introduce W^* – the space of currents dual to the space W, that is, the space of continuous linear mappings: $W \to \mathbb{R}$. For any current $T_S(\cdot) \in W^*$, there is such a representation $K^W T_S \in W$ that $T_S(\omega) = \langle K^W T_S, \omega \rangle_W$, $\forall \omega \in W$. The space W is a vector-valued RKHS (see Appendix 1), W equipped with an inner product $\langle K^W(\cdot, x)\alpha, K^W(\cdot, y)\beta \rangle_W = \alpha^T K^W(x, y)\beta$, that is defined for the fields $K^W(\cdot, x)\alpha$ and $K^W(\cdot, y)\beta$. If we denote $K^W(\cdot, y)\beta$ as ω, then we obtain the reproducing property: $\langle K^W(\cdot, x)\alpha, \omega \rangle_W = \alpha^T \omega(x)$; $\forall \omega \in W$.

There is a linear mapping: $L_W\colon W \to W^*$, between space W and the corresponding space of currents: $W^*\colon L_W(\omega)(\omega') = \langle \omega, \omega' \rangle_W$, $\forall \omega, \omega' \in W$. The inner product $\langle \cdot, \cdot \rangle_W$ can be mapped to the current space W^* using linear mapping L_W. Then the inner product is between two currents T, T': $\langle T, T' \rangle_{W^*} = \langle L_W^{-1}(T), L_W^{-1}(T') \rangle_W$.

In space W, the basic elements are fields of the form $K^W(\cdot, x)\alpha$, and the corresponding basic elements in space W^* are the Dirac δ-currents: $\delta_x^\alpha = L_W^{-1}\left(K^W(\cdot, x)\alpha\right)$. From the definition δ_x^α and L_W we get: $\delta_x^\alpha(\omega) = \langle K^W(\cdot, x)\alpha, \omega \rangle_W = \alpha^T \omega(x)$. Inner product between Dirac δ-currents:

$$\left\langle \delta_x^\alpha, \delta_y^\beta \right\rangle_{W^*} = \langle K(\cdot, x)\alpha, K(\cdot, y)\beta \rangle_W = \alpha^T K^W(x, y)\beta.$$

If the current T represents a curve (or surface), then it can be decomposed into many tangents (normals). The dual representation $\mathcal{L}_W^{-1}(T)$ of the current (vector field in W) is the convolution of all tangents (normals) with the kernel K^W. Polygons of the curve (surface mesh) can be approximated by a finite sum: $T \sim \sum\limits_k \delta_{x_k}^{\alpha_k}$, where x_k is the center of each segment (mesh cell) and α_k is the tangent (normal to the surface) at the point x_k. The value α_k encodes the size of the segment (surface mesh). The dual representation of the current at any point x is given by the sum: $\sum\limits_k K^W(x, x_k)\alpha_k$. The integrals of currents in the discrete approximation are replaced by the sums for the curves: $T_l(\omega) \sim \sum\limits_k \omega(x_k)^T \tau_k$, where τ_k is the tangent at a point x_k; for surfaces: $T_S(\omega) \sim \sum\limits_k \omega(x_k)^T n_k$, where n_k is the normal to the surface at a point x_k.

4. The distance between the shapes of objects

The inner product between two sets of Dirac currents: $T = \sum\limits_i \delta_{x_i}^{\alpha_i}$, $T' = \sum\limits_j \delta_{y_j}^{\beta_j}$, can be determined from the relation: $\left\langle T, T' \right\rangle_{W^*} = T L_W^{-1} T' = \sum\limits_i \sum\limits_j \alpha_i^T K^W(x_i, y_j)\beta_j$.

We define the square of the distance between two shapes simulated by currents:

$$
\begin{aligned}
d\left(T, T'\right)^2 &= \left\| T - T' \right\|_{W^*}^2 = \left(T - T'\right) L_W^{-1} \left(T - T'\right) = \\
&= \sum_{p=1}^{N} \sum_{q=1}^{N} \alpha_{xp}^T K^W \left(x_p, x_q\right) \alpha_{xq} - \\
&-2 \sum_{p=1}^{N} \sum_{q=1}^{N} \alpha_{xp}^T K^W \left(x_p, y_q\right) \alpha_{yq} + \sum_{p=1}^{N} \sum_{q=1}^{N} \alpha_{yp}^T K^W \left(y_p, y_q\right) \alpha_{yq},
\end{aligned}
\tag{2}
$$

where $K^W\left(x_p, x_q\right) = \exp\left(-\left\|x_p - x_q\right\|^2 \lambda_W^{-2}\right)$. To take into account the diffeomorphic deformation of the source shape, it is necessary to add the functional J_0 multiplied by the regularization coefficient to the squared distance $d\left(T, T'\right)^2$.

If the curve l is given by simplicial complexes with points $(x_1, y_1), \ldots, (x_N, y_N), (x_{N+1}, y_{N+1})$, then the centers of the segments between adjacent points of the corresponding complexes: $c_{xi} = \frac{(x_i + x_{i+1})}{2}$, $c_{yi} = \frac{(y_i + y_{i+1})}{2}$, and the tangents formed by these segments: $\alpha_{xi} = \frac{(x_{i+1} - x_i)}{2}$, $\alpha_{yi} = \frac{(y_{i+1} - y_i)}{2}$; $i = 1, 2, \ldots, N$. Then: $l \rightarrow T_l(\omega) \sum_{j=1}^{N} K\left(c_j, \cdot\right)\left(\alpha_j\right)$. If S is an oriented triangulated surface defined by points: $(x_1, y_1, z_1), \ldots, (x_N, y_N, z_N), (x_{N+1}, y_{N+1}, z_{N+1})$, where each j-th triangle is represented by the center: $c_{x_j} = \frac{(x_j + x_{j+1} + x_{j+2})}{3}$, $c_{y_j} = \frac{(y_j + y_{j+1} + y_{j+2})}{3}$, $c_{z_j} = \frac{(z_j + z_{j+1} + z_{j+2})}{3}$, and by a normal vector n_j to the j-th triangle, whose norm encodes the area of the triangle. Then: $S \rightarrow T_S(\omega) \sum_{j=1}^{N} K\left(x_j, \cdot\right)\left(n_j\right)$.

If the set $\left(x_p, \alpha_p\right)_{p=1\ldots N}$ contains functions f_{x_p} representing signals at the points x_p: $\left(x_p, \alpha_p, f_{x_p}\right)_{p=1\ldots N}$, then the square of the distance $\left\| T - T' \right\|_{W^*}^2$ in (2) can be represented as:

$$
\begin{aligned}
d\left(T, T'\right)^2 &= \left\| T - T' \right\|_{W^*}^2 = \sum_{p=1}^{N} \sum_{q=1}^{N} K^f\left(f_{x_p}, f_{x_q}\right) \cdot \alpha_{xp}^T K^W\left(x_p, x_q\right) \alpha_{xq} - \\
&-2 \sum_{p=1}^{N} \sum_{q=1}^{N} K^f\left(f_{x_p}, f_{y_q}\right) \cdot \alpha_{xp}^T K^W\left(x_p, y_q\right) \alpha_{yq} + \\
&+ \sum_{p=1}^{N} \sum_{q=1}^{N} K^f\left(f_{y_p}, f_{y_q}\right) \cdot \alpha_{yp}^T K^W\left(y_p, y_q\right) \alpha_{yq},
\end{aligned}
\tag{3}
$$

where: $K^f\left(f_{x_p}, f_{x_q}\right) = \exp\left(-\left(f_{x_p} - f_{x_p}\right)^2 \lambda_f^{-2}\right)$, λ_f is the standard deviation f_{x_p} in the space of functions.

4.1. Example 1

Consider an example of matching the shapes of objects. Let a simplicial complex with a set of points $x_1, \ldots, x_n$ be given. If the complex is approximated by a curve, then the centers of the segments and the tangents have the form: $c_i = \frac{(x_i + x_{i+1})}{2}$, $\alpha_i = \frac{(x_{i+1} - x_i)}{2}$, respectively.

Let us consider a matching of the shapes of objects: a square T with vertices: $x = \left(\binom{1}{1}, \binom{-1}{1}, \binom{-1}{-1}, \binom{1}{-1}\right)$, centers of edges: $c^x = \left(\binom{0}{1}, \binom{-1}{0}, \binom{0}{-1}, \binom{1}{0}\right)$, covectors corresponding to tangents to edges: $\alpha^x = \left(\binom{-1}{0}^T, \binom{0}{-1}^T, \binom{1}{0}^T, \binom{0}{1}^T\right)$, and a triangle T' with vertices: $y = \left(\binom{0}{1}, \binom{-\frac{\sqrt{3}}{2}}{-\frac{1}{2}}, \binom{\frac{\sqrt{3}}{2}}{-\frac{1}{2}}\right)$, centers of edges: $c^y = \left(\binom{-\frac{\sqrt{3}}{4}}{\frac{1}{4}}, \binom{0}{-\frac{1}{2}}, \binom{\frac{\sqrt{3}}{4}}{\frac{1}{4}}\right)$, covectors corresponding to tangents to edges: $\beta^y = \left(\binom{-\frac{\sqrt{3}}{4}}{-\frac{3}{4}}^T, \binom{\frac{\sqrt{3}}{2}}{0}^T, \binom{-\frac{\sqrt{3}}{4}}{\frac{3}{4}}^T\right)$.

The square of the distance $d\left(T, T'\right)^2 = \left\| T - T' \right\|_{W^*}^2$ with $\lambda_V = 1$, according to (2), is equal to $d\left(T, T'\right)^2 = 1,748$. If there are functions f_{x_p} representing signals at the vertices x_p:

$f_{x_1} = 1, f_{x_2} = 2, f_{x_3} = 3, f_{x_4} = 4$; and the functions f_{y_p} representing the signals in y_p: $f_{y_1} = 1, f_{y_2} = 2, f_{y_3} = 3$, are included in the sets $\left(x_p, \alpha_p\right)_{p=1\dots4}$ and $\left(y_{p'}, \beta_{p'}\right)_{p'=1\dots3}$, then the square of the distance $d\left(T, T'\right)^2 = \left\|T - T'\right\|^2_{W^*}$ with $\lambda_f = 1$, according to (3), is equal $d\left(T, T'\right)^2 = 1,966$.

4.2. Example 2

Let us consider an example of a diffeomorphic deformation of the image shape of a symbol of an indefinite shape into an image shape of the shape of number 2 (Fig. 1), number 7 (Fig. 2) and number 8 (Fig. 3).

The evolution of deformations of a diffeomorphic shape was determined based on the solution of equations (1). The functional is minimized by values using the QPSO algorithm (see Appendix 2, [18]). In fig. 1, 2, 3 shows intermediate shapes of images for times: $t = 0$ (source image shape), $t = 0,5$ (intermediate image shape), $t = 1$ (terminal image shape).

(a) $t = 0$ (b) $t = 0,5$ (c) $t = 1$
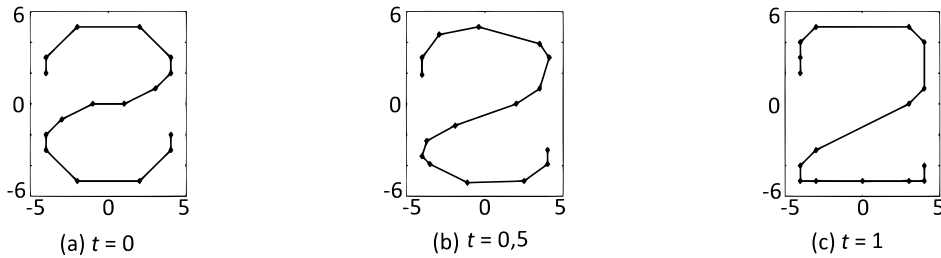
Fig. 1. Deformation of the shape of the symbol in the shape of number 2

Fig 1. Деформация формы символа в форму цифры 2

(a) $t = 0$ (b) $t = 0,5$ (c) $t = 1$
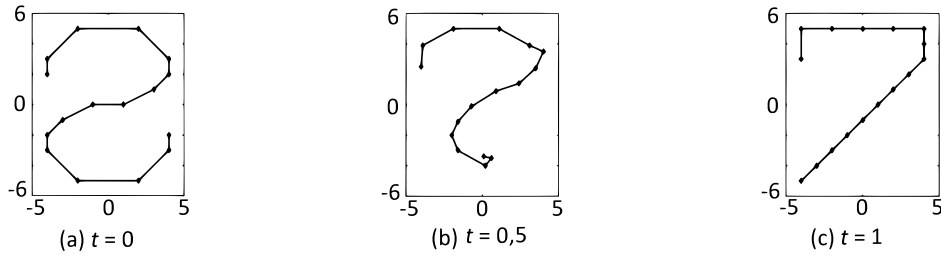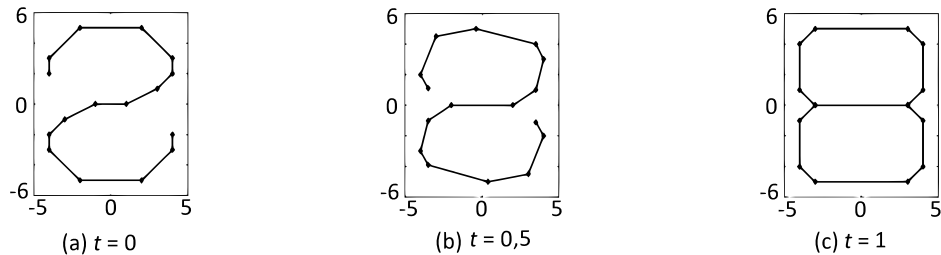
Fig. 2. Deformation of the shape of the symbol in the shape of number 7

Fig 2. Деформация формы символа в форму цифры 7

(a) $t = 0$ (b) $t = 0,5$ (c) $t = 1$

Fig. 3. Deformation of the shape of the symbol in the shape of the number 8

Fig 3. Деформация формы символа в форму цифры 8

In this case, the values of the squared distance between the source image and the terminal shape $d^2\left(T, T'\right)$, determined from relation (2) with $\lambda_W = 1$, are:

- for the case of deformation of the shape of the symbol in the shape of numbers 2: $d^2\left(T, T'\right) = 78, 6$;
- for the case of deformation of the shape of the symbol in the shape of the number 7: $d^2\left(T, T'\right) = 78, 0$;
- for the case of deformation of the shape of the symbol in the shape of the figure 8: $d^2\left(T, T'\right) = 16, 8$.

Therefore, the algorithm recognizes the character as the number 8.

It should be noted that during deformation of the shape of the symbol into the shape of the figure 8, the topological genus of the shape changes from 0 to 1, that is, the deformation is not a diffeomorphism, but a metamorphosis.

5. Normalization of images based on affine transformations

To improve the accuracy of matching of source and terminal images, these images should be normalized. Below we propose such a normalization method, in which the original image undergoes affine transformation and the functional between the converted original and terminal images is minimized. After that, the normalized original image undergoes a diffeomorphic transformation, while the distance (2) between the converted and terminal images is reduced, which will increase the accuracy of the matching.

An affine transformation is a special case of a diffeomorphic transformation. An affine transformation can be represented in the form [19]:

$$\mathbf{x} \longrightarrow \mathbf{y} = \mathbf{M} \cdot \mathbf{x} + \mathbf{b},$$

where $\mathbf{M} \in \mathbb{R}^{n \times n}$ is an invertible matrix, $\mathbf{b} \in \mathbb{R}^n$, x, y are vectors in an affine space $X \in \mathbb{R}^n$.

In the case of an affine transformation of a curve (surface) point p approximating the shape of a deformable object, it can be represented as: $\mathbf{y}_p \longrightarrow \mathbf{M} \cdot \mathbf{x}_p + \mathbf{b}$, $p = 1, \dots, P$. As the minimized functional, we choose the square of the distance between the points of the source and final images: $J\left(\mathbf{M}, \mathbf{b}\right) = d\left(T, T'\right)^2$, where $d\left(T, T'\right)^2$ it is determined in accordance with (2), T is the current corresponding to the initial shape of the object, T' is the current corresponding to the shape of the deformable object after affine transformation. Let ξ^j be the parameters of the affine transformation: $\xi^j \in \Xi; j = 1, \dots, N$, where Ξ, is the set of matrix components $\mathbf{M}$ and vector components $\mathbf{b}$.

The values of the parameters ξ_i of the particle i can be found using the QPSO algorithm (quantum particle swarm optimization, see Appendix 2, [18]) to minimize the functional $J\left(\Xi\right)$. We denote the value of the minimized functional E_n on the set: $\xi_{i,n}^j \in \Xi$: $E_n = J\left(\xi_{1,n}^j, \dots, \xi_{I,n}^j\right)$, where n is the iteration step number, and $i \in [1 \dots I]$ is the particle number. Let $P_{i,n}$ be the values of the parameters that provide the smallest value of the functional E_n for the particle i after the n-th iteration, and G_n be the values of the parameters that provide the smallest value of the functional E_n for all particles after the n-th iteration. We choose the values of the best values of the parameters from the relation:

$$p_{i,n} = \phi_{i,n} \cdot P_{i,n} + (1 - \phi_{i,n}) \cdot G_n,$$

where $\phi_{i,n} \in [0 \dots 1]$ is a random number of a uniform distribution. The parameters ξ_i of the particle i at the next iteration step $(n + 1)$ can be determined from the relation:

$$\begin{aligned}
&\text{if } (\psi_{i,n} < 0, 5) \text{ then } \xi_{i,n+1}^j = p_{i,n}^j - \beta \cdot \left|\xi_{i,n}^j - p_{i,n}^j\right| \cdot \ln\left(u_{i,n+1}^j\right); \\
&\text{else } \xi_{i,n+1}^j = p_{i,n}^j + \beta \cdot \left|\xi_{i,n}^j - p_{i,n}^j\right| \cdot \ln\left(u_{i,n+1}^j\right),
\end{aligned} \quad (4)$$

where $\psi_{i,n} \in [0 \dots 1]$, $u_{i,n}^j \in [0 \dots 1]$ are random numbers of uniform distribution.
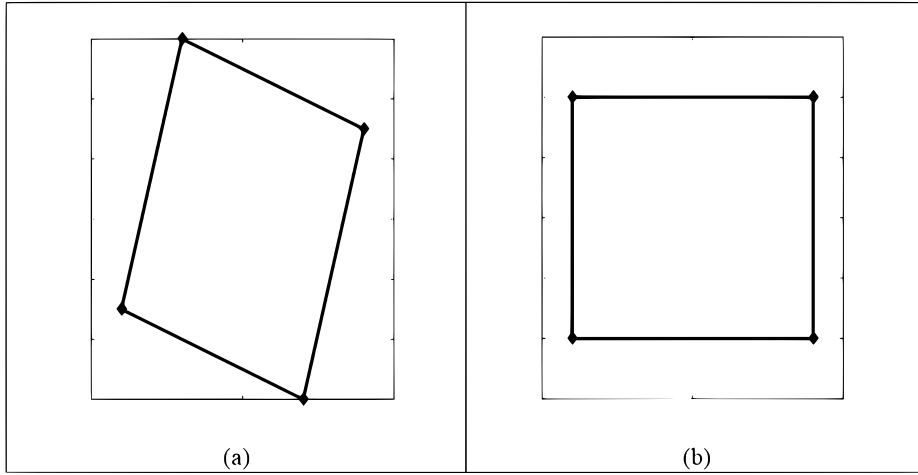
Fig. 4. Example of affine transformation   **Fig 4.** Пример аффинного преобразования

5.1. Example 3

Consider the example of the affine transformation of a quadrangle T with vertices $\mathbf{x} = \left(\begin{pmatrix} -4 \\ -3 \end{pmatrix} \begin{pmatrix} -2 \\ 6 \end{pmatrix} \begin{pmatrix} 4 \\ 3 \end{pmatrix} \begin{pmatrix} 2 \\ -3 \end{pmatrix} \right)$, into a square T' with vertices $\mathbf{x} = \left(\begin{pmatrix} 4 \\ 4 \end{pmatrix} \begin{pmatrix} 4 \\ -4 \end{pmatrix} \begin{pmatrix} -4 \\ -4 \end{pmatrix} \begin{pmatrix} -4 \\ 4 \end{pmatrix} \right)$: $\mathbf{x} \longrightarrow \mathbf{y} = \mathbf{M} \cdot \mathbf{x} + \mathbf{b}$; (see fig. 4).

Before the affine transformation, the value $d\left(T, T'\right)$ (see (2)) is equal $d\left(T, T'\right) = 8, 2$. After carrying out the affine transformation and minimizing the distance $d\left(T, T'\right)$, we obtain the required components of the matrix $\mathbf{M}$: $\mathbf{M} = \begin{pmatrix} 1,2 & -0,26 \\ 0,38 & 0,8 \end{pmatrix}$, and the vector $\mathbf{b}$: $\mathbf{b} = \begin{pmatrix} 0 & 0 \end{pmatrix}^T$. Preliminary affine transformation reduced the distance to $d\left(T, T'\right) = 0, 67$.

Conclusion

The paper considered an algorithm for matching image shapes, based on the de Rham currents method and preliminary affine transformation of the source image shape. The de Rham current method can be used to represent shapes of various nature: point landmarks, curves, surfaces, signals. Using the proposed matching algorithm allows us to solve the problem of ensuring invariance to geometric transformations of images and ensuring the absence of a bijective correspondence requirement between image segments. The algorithm for matching shapes based on the current method is stable when changing the topology of the shapes of objects and changing parameterization. An application of the method of reproducing kernel Hilbert space (RKHS) to obtain metrics of the shape of an object is proposed.

To increase the accuracy of matching the shapes of the source and terminal images, it is proposed that the source image be subjected to preliminary affine transformation. The problem of invariance to geometric transformations of images (translation, rotation, scaling, skew) is solved. The minimization of the functional of the squared distance between the image shapes is based on the QPSO algorithm.

The results of a diffeomorphic matching of the shapes of objects with the extension of the LDDMM (large deformation diffeomorphic metric mapping) algorithm to the case of metamorphosis, in which there may be a bijective correspondence between the segments of the source and terminal images, are presented. To improve the accuracy of matching the shapes of the source and terminal images, we determine the functional on the basis of the formation of a squared distance between the shapes of the source and terminal images modeled by de Rham currents.

Appendix 1. Reproducing kernel Hilbert spaces

RKHS (reproducing kernel Hilbert spaces) is a Hilbert space of functions in which a point esti-mation is a continuous linear functional [11]. If two functions in RKHS are close in norm: $\|f - g\| \to 0$, then $|f(x) - g(x)| \to 0; \forall x$. For kernel $k(x, x')$, we construct a Hilbert space so that $k(x, x')$ is a scalar product in this space. For given points $x_1, x_2, ..., x_n$, we define the Gram matrix: $K_{ij} = k(x_i, x_j)$. We say that a kernel is positive definite if its Gram matrix is positive definite for all $x_i, x_j; i, j = 1, ..., n$. We define a linear functional L_x in a Hilbert space H that estimates each function at a point x: $L_x : f \to f(x), \forall f \in H$. Space H is generated by the reproducing kernel, if $L_x(f)$ is a continuous function for all $x \in X$. The estimation of functional L_x can be represented by taking the inner product of the function f with the function of the reproducing kernel $k(\cdot, x) \in H$. Define a map $\Phi : x \to k(\cdot, x)$. i.e. with each point x in the source space we associate a function $k(\cdot, x)$ with a reproducing property: $f(x) = L_x(f) = \langle f, \ k(\cdot, x) \rangle; \ \forall f \in H, \forall x \in X$. Since $k(\cdot, x) \in H$, then: $k(y, x) = L_y(k(\cdot, x)) = \langle k(\cdot, x), k(\cdot, y) \rangle$, where $k(\cdot, y) \in H$ is the element associated with L_y. This allows us to define the reproducing kernel for H as a function $K : X \times X \to \mathbb{R}$: $k(x, y) = \langle k(\cdot, x), k(\cdot, y) \rangle$. We construct a vector space RKHS containing all linear combinations of functions $k(\cdot, x) : f(\cdot) = \sum_{j=1}^{m} \alpha_i k(\cdot, x_i)$. Let be: $g(\cdot) = \sum_{j=1}^{m'} \beta_j k(\cdot, x_j')$; define the inner product:

$$\langle f, g \rangle = \sum_{i=1}^{m} \sum_{j=1}^{m'} \alpha_i \beta_j k(x_i, x_j').$$

For any function: $f(\cdot) = \sum_{j=1}^{m} \alpha_i k(\cdot, x_i)$, the following relation is valid:

$$\langle k(\cdot, x), f \rangle = \sum_{i=1}^{m} \alpha_i k(x_i, x) = f(x).$$

The kernels are analogues of Dirac δ-functions. In space L_2:

$$\langle \delta(\cdot, x), f \rangle = \int f(t) \delta(t, x) \, dt = f(x),$$

where $\delta(t, x)$ is the Dirac δ-function.

Appendix 2.
Quantum particle swarm optimization algorithm

The PSO algorithm is presented in [20]. The PSO algorithm considers a set of particles; each particle is a suitable solution to the optimization problem. In terms of classical mechanics, a particle is represented by a vector of its position and a velocity vector, which determine the trajectory of the particle. In quantum mechanics, the term "trajectory" does not make sense, since, in accordance with the principle of uncertainty, the coordinates and velocities of particles cannot be deter-mined simultaneously. A model with a quantum-mechanical potential well based on E. Schrödinger equation [18] is considered below. In quantum mechanics, the state of a particle is deter-mined by the wave function $\psi(x, t)$. In one-dimensional space, the wave function of a particle determines $Q(x, t)$: $|\psi(x, t)|^2 dx = Q(x, t) dx$, where $Q(x, t) dx$ is the probability that a measurement of the particle's position at a certain point in time will find it in a neighborhood relative to a point x with the volume of the neighborhood dx. The probability density function satisfies the relation:

$$\int_{-\infty}^{\infty} |\psi|^2 \, dx = \int_{-\infty}^{\infty} Q dx = 1.$$

The wave function $\psi(x, t)$ changes in time in accordance with E. Schrödinger equation: $i\hbar \frac{\partial}{\partial t} \psi(x, t) = \hat{H} \psi(x, t)$. For a particle of mass m in a potential field $V(x)$, the Hamilton operator $\hat{H}$ is given by the formula: $\hat{H} = -\frac{\hbar^2}{2m} \nabla^2 + V(x)$, where $\hbar$ is Planck's constant.

Suppose that each particle moves in an δ-potential well in the search space whose center is a point p. The potential energy of a particle in a one-dimensional δ-potential well is represented in the form: $V(x) = -\gamma \cdot \delta(x - p)$. Let be: $y = x - p$. Solving the Schrödinger equation for $y \neq 0$, we obtain the probability density function:

$$Q(y) = |\psi(y)|^2 = L^{-1} \exp\left(-2 |y| L^{-1}\right),$$

where L is the characteristic "length" of the δ-potential well. Let s be a uniformly distributed random number: $s = L^{-1} u$; $u = \text{rand}(0, 1)$. Replacing $|\psi(y)|^2$ with s, we get: $s = L^{-1} \cdot \exp\left(-2 |y| L^{-1}\right)$; $y = x - p = \pm \frac{L}{2} \ln\left(u^{-1}\right)$, consequently: $x = p \pm \frac{L}{2} \ln\left(u^{-1}\right)$. We form L at the k-th step of the iteration: $L = \beta \cdot |x_k - p|$, where β is the parameter that controls the search process.

Let $P_{i,n}$ be the values of the parameters that provide the smallest value of the functional E_n for the particle i after the n-th iteration, and G_n be the values of the parameters that provide the smallest value of the functional E_n for all particles after the n-th iteration. We choose the values of the best values of the parameters from the relation: $p_{i,n} = \phi_{i,n} \cdot P_{i,n} + (1 - \phi_{i,n}) \cdot G_n$, where $\phi_{i,n} \in [0 \ldots 1]$ is a random number of a uniform distribution. The parameters ξ_i of the particle i at the next iteration step $(n + 1)$ can be determined from the relation:

$$\text{if } (\psi_{i,n} < 0, 5) \text{ then } \xi_{i,n+1}^j = p_{i,n}^j - \beta \cdot \left|\xi_{i,n}^j - p_{i,n}^j\right| \cdot \ln\left(u_{i,n+1}^j\right);$$
$$\text{else } \xi_{i,n+1}^j = p_{i,n}^j + \beta \cdot \left|\xi_{i,n}^j - p_{i,n}^j\right| \cdot \ln\left(u_{i,n+1}^j\right),$$

where $\psi_{i,n} \in [0 \ldots 1]$, $u_{i,n}^j \in [0 \ldots 1]$ are random numbers of uniform distribution.

References

[1] K. Grauman and B. Leibe, "Visual object recognition", *Synthesis lectures on artificial intelligence and machine learning*, vol. 5, no. 2, pp. 1–181, 2011.

[2] A. Goshtasby, *Theory and applications of image registration*. John Wiley & Sons, 2017.

[3] D. Zhang, G. Lu, and L. Zhang, *Advanced biometrics*. Springer, 2018.

[4] M. Miller, A. Trouvé, and L. Younes, "Hamiltonian systems and optimal control in computational anatomy: 100 years since D'Arcy Thompson", *Annual review of biomedical engineering*, vol. 17, pp. 447–509, 2015.

[5] M. Deza and E. Deza, "Encyclopedia of distances", in *Encyclopedia of distances*, Springer-Verlag Berlin Heidelberg, 2016.

[6] L. Younes, *Shapes and diffeomorphisms*. Springer-Verlag Berlin Heidelberg, 2019, vol. 171.

[7] G. De Rham, F. Smith, and S. Chern, *Differentiable manifolds: forms, currents, harmonic forms*. Springer-Verlag, 1984, vol. 266.

[8] S. Chukanov, "A rotation, translation, and scaling invariant Fourier transform of 3D image function", *Optoelectronics, Instrumentation and Data Processing*, vol. 44, no. 3, pp. 249–255, 2008.

[9] S. Chukanov, "Constructing invariants for visualization of vector fields defined by integral curves of dynamic systems", *Optoelectronics, Instrumentation and Data Processing*, vol. 47, no. 2, pp. 151–155, 2011.

[10] S. Chukanov, "Comparison of objects' images based on computational topology methods", *Trudy SPIIRAN*, vol. 18, no. 5, pp. 1043–1065, 2019.

[11] N. Aronszajn, "Theory of reproducing kernels", *Trans. Amer. Math. Soc.*, vol. 68, no. 3, pp. 337–404, 1950.

[12] C. Micchelli and M. Pontil, "On learning vector-valued functions", *Neural computation*, vol. 17, no. 1, pp. 177–204, 2005.

[13] J. Glaunes and M. Micheli, "Matrix-valued kernels for shape deformation analysis. Geometry", *Imaging and Computing*, vol. 1, no. 1, pp. 57–139, 2014.

[14] S. Lejhter and S. Chukanov, "Matching of images based on their diffeomorphic mapping", *Computer optics*, vol. 42, no. 1, pp. 96–104, 2018.

[15] S. Barahona, X. Gual-Arnau, M. Ibá nez, and A. Simó, "Unsupervised classification of children?s bodies using currents", *Advances in Data Analysis and Classification*, vol. 12, no. 2, pp. 365–397, 2018.

[16] I. Kaltenmark, B. Charlier, and N. Charon, "A general framework for curve and surface comparison and registration with oriented varifolds", in *Proceedings of the IEEE Conference on Computer Vision and Pattern Recognition*, 2017, pp. 3346–3355.

[17] M. Vaillant and J. Glaunès, "Surface matching via currents", in *Biennial International Conference on Information Processing in Medical Imaging*, Springer, 2005, pp. 381–392.

[18] D. Tang, Y. Cai, J. Zhao, and Y. Xue, "A quantum-behaved particle swarm optimization with memetic algorithm and memory for continuous non-linear large scale problems", *Information Sciences*, vol. 289, pp. 162–189, 2014.

[19] J. Flusser, B. Zitova, and T. Suk, *Moments and moment invariants in pattern recognition*. John Wiley & Sons, 2009.

[20] J. Kennedy and R. Eberhart, "Particle swarm optimization", in *Proceedings of ICNN'95-International Conference on Neural Networks*, IEEE, vol. 4, 1995, pp. 1942–1948.